Point Mutations in Apolipoprotein A-I Mimic the Phenotype Observed in Patients with Classical Lecithin:Cholesterol Acyltransferase Deficiency†

Angeliki Chroni, Adelina Duka, Horng-Yuan Kan, Tong Liu, and Vassilis I. Zannis*

Molecular Genetics, Whitaker Cardiovascular Institute, Departments of Medicine and Biochemistry, Center for Advanced Biomedical Research, Boston University School of Medicine, Boston, Massachusetts 02118

Received May 24, 2005; Revised Manuscript Received August 4, 2005

ABSTRACT: We have analyzed the effect of charged to neutral amino acid substitutions around the kinks flanking helices 4 and 6 of apoA-I and of the deletion of helix 6 on the in vivo activity of LCAT and the biogenesis of HDL. The LCAT activation capacity of apoA-I in vitro was nearly abolished by the helix 6 point (helix 6P-apoA-I[R160V/H162A]) and deletion {helix 6Δ-apoA-I[Δ(144−165)]} mutants, but was reduced to 50% in the helix 4 point mutant (helix 4P-apoA-I[D102A/D103A]). Following adenovirus-mediated gene transfer in apoA-I deficient mice, the level of plasma HDL cholesterol was greatly reduced in helix 6P and helix 6Δ mutants. Electron microscopy and two-dimensional gel electrophoresis showed that the helix 6P mutant formed predominantly high levels of apoA-I containing discoidal particles and had an increased preβ1-HDL/α-HDL ratio. The helix 6Δ mutant formed few spherical particles and had an increased preβ1-HDL/α-HDL ratio. Mice infected with adenovirus expressing the helix 4P mutant or wild-type apoA-I had normal HDL cholesterol and formed spherical α-HDL particles. Coinfection of mice with adenoviruses expressing human LCAT and the helix 6P mutant dramatically increased plasma HDL and apoA-I levels and converted the discoidal into spherical HDL, indicating that the LCAT activity was rate-limiting for the biogenesis of HDL. The LCAT treatment caused only a small increase in HDL cholesterol and apoA-I levels and in α-HDL particle numbers in the helix 6Δ mutant. The findings indicate a critical contribution of residue 160 of apoA-I to the in vivo activity of LCAT and the subsequent maturation of HDL and explain the low HDL levels in heterozygous subjects carrying this mutation.

Apolipoprotein A-I (apoA-I)[1] is the major protein component of HDL, and plays an essential role in the biogenesis and the functions of HDL (*1*−*4*). ApoA-I contains 22- and 11-amino acid repeats (*5*) which, based on X-ray crystallography (*6*) and physicochemical studies (*5*), are organized predominantly in amphipathic α-helices. This unique apoA-I structure may underlie several of its functions. On the basis of the crystal structure and several structural studies, detailed belt as well as hairpin-shaped models have been proposed that describe the binding of apoA-I in discoidal and spherical HDL particles (*7*, *8*).

It is generally believed that the biogenesis of HDL occurs through a complex pathway that requires apoA-I and several other proteins (*4*).

In the early steps of this pathway, apoA-I is secreted mostly lipid free by the liver and acquires phospholipid and cholesterol via its interactions with the ATP-binding cassette A1 (ABCA1) lipid transporter (*1*, *9*). Through a series of intermediate steps that are poorly understood, apoA-I is gradually lipidated and proceeds to form discoidal particles which are converted to spherical particles by the action of lecithin:cholesterol acyltransferase (LCAT) (*2*, *10*). Both the discoidal and spherical HDL particles interact functionally with the HDL receptor scavenger receptor class B type I (SR-BI) (*3*, *11*, *12*). The late steps of the HDL pathway involve the transfer of cholesteryl esters to VLDL or LDL for eventual catabolism by the LDL receptor, the hydrolysis of phospholipids and residual triglycerides by the various lipases (lipoprotein lipase, hepatic lipase, and endothelial lipase), and the transfer of phospholipids from VLDL and LDL to HDL by the action of phospholipid transfer protein (*13*).

Biogenesis of HDL is prevented by apoA-I deficiency or mutations in ABCA1 that diminish the functional interactions with ABCA1 (*1*, *9*, *14*). In addition, formation and/or maturation of HDL is prevented by mutations in LCAT or mutations in apoA-I which prevent the activation of LCAT (*15*, *16*). The domains of apoA-I involved in LCAT activation were initially studied by analysis of natural and

† This work was supported by National Institutes of Health Grants HL-33952 and HL-48739 and KOS Pharmaceuticals (Miami, FL).

* To whom correspondence should be addressed: Whitaker Cardiovascular Institute, Center for Advanced Biomedical Research, Boston University School of Medicine, 715 Albany St., Boston, MA 02118. Telephone: (617) 638-5085. Fax: (617) 638-5141. E-mail: vzannis@bu.edu.

[1] Abbreviations: ABCA1, ATP-binding cassette transporter A1; apoA-I, apolipoprotein A-I; apoA-I$^{-/-}$ mice, apoA-I-deficient mice; EM, electron microscopy; CE, cholesteryl esters; FC, free cholesterol; GFP, green fluorescence protein; HDL, high-density lipoproteins; helix 4P, helix 4 point mutant apoA-I[D102A/D103A]; helix 6P, helix 6 point mutant apoA-I[R160V/H162A]; helix 6Δ, helix 6 deletion mutant apoA-I[Δ(144−165)]; IDL, intermediate-density lipoproteins; LCAT, lecithin:cholesterol acyltransferase; LDL, low-density lipoproteins; PBS, phosphate-buffered saline; PL, phospholipids; POPC, β-oleoyl-γ-palmitoyl-L-α-phosphatidylcholine; SR-BI, scavenger receptor class B type I; VLDL, very low-density lipoproteins; TC, total cholesterol; TG, triglycerides; WT, wild-type.

10.1021/bi050962o CCC: $30.25
Published on Web 10/07/2005

bioengineered apoA-I mutants. The in vitro studies suggested that although several regions of apoA-I may contribute to the activation of LCAT, specific residues within helix 6 may be essential for LCAT activation (*17*−*24*). Few studies have investigated the effect of apoA-I mutations on the biogenesis of HDL. In vivo analysis of deletion mutants showed that deletions of either helices 4 and 5 {apoA-I[Δ(100−143)]}, helices 5 and 6 {apoA-I[Δ(122−165)]}, or helices 6 and 7 {apoA-I[Δ(144−186)]} resulted in very low apoA-I and HDL levels following adenovirus-mediated gene transfer in apoA-I deficient (apoA-I$^{-/-}$) mice and led to the formation of discoidal HDL particles (*25*).

Similar studies of amino-terminal deletion mutants apoA-I[Δ(7−43)] and apoA-I[Δ(7−65)] also showed that both these mutations were associated with low plasma apoA-I and HDL levels following adenovirus-mediated gene transfer in apoA-I$^{-/-}$ mice. The deletion of residues 7−43 resulted in the generation of spherical HDL particles, whereas the deletion of residues 7−65 resulted in the generation of discoidal HDL particles. The findings indicate that the amino terminus of apoA-I also plays some role in the activation of LCAT in vivo (*26*). Impairment of LCAT activation and accumulation of discoidal HDL particles following adenovirus-mediated gene transfer of an apoA-I mutant lacking residues 89−99 in apoA-I$^{-/-}$ mice were also observed (*27*).

Transgenic mice expressing apoA-I[Δ(143−164)] in an apoA-I$^{-/-}$ background had greatly reduced apoA-I and HDL plasma levels based on FPLC analysis and generated cholesteryl ester poor HDL particles 8 nm in diameter (*23*). Overall, the experiments in transgenic mice and following adenovirus-mediated gene transfer of the truncated apoA-I forms in apoA-I$^{-/-}$ mice identified the regions of apoA-I that affect LCAT activation in vivo. However, the large deletions introduced in these studies may have altered drastically the apoA-I structure, and thus necessitate that the involvement of specific residues, within these regions, in LCAT activation is further validated by targeted in vitro mutagenesis and functional analyses.

For this purpose, we have used adenovirus-mediated gene transfer in apoA-I$^{-/-}$ mice to assess the role of the carboxy-terminal amino acids of apoA-I in the assembly and metabolism of HDL (*28*). These analyses showed that substitution of hydrophobic residues in the region of residues 211−229 with either charged or less bulky hydrophobic residues resulted in low levels of HDL and formation of discoidal HDL particles following gene transfer of mutant apoA-I forms in apoA-I$^{-/-}$ mice. In contrast, substitution of charged residues 234−239 with Ala led to the formation of normal HDL (*28*). The data showed for the first time that defective maturation of HDL may occur in vivo as a result of specific point mutations in apoA-I.

We have also shown, by analysis of several apoA-I mutants, that charged to neutral amino acid substitutions around the kinks flanking helices 4 and 6 of apoA-I have a profound effect on the functional interactions of lipid-bound apoA-I with WT and mutant SR-BI forms (*3*, *29*). Other studies have shown that natural mutations around residues R160 and H162 of apoA-I as well as deletions in helix 6 or 7 of apoA-I are associated with low HDL levels and/or have reduced capacity to activate LCAT in vitro (*15*, *30*−*37*).

Here we analyzed the impact of point mutations in helices 4 and 6 and the deletion of helix 6 of apoA-I on the biogenesis of HDL and the activity of LCAT in vivo using adenovirus-mediated gene transfer of apoA-I mutants in apoA-I$^{-/-}$ mice. The formation of HDL was assessed by FPLC fractionation, EM analysis, and two-dimensional gel electrophoresis of plasma. The in vivo capacity of the endogenous enzyme to activate LCAT was assessed from the CE/TC ratio of the HDL fraction and the restoration of the CE/TC ratio and the plasma HDL levels by coinfection of mice with adenoviruses expressing the mutant apoA-I forms and human LCAT. It was found that although both the helix 6 point mutant (apoA-I[R160A/H162A]) and the deletion mutant {apoA-I[Δ(144−165)]} affected the activity of LCAT in vitro and in vivo and the biogenesis of HDL in vivo, only the defect caused by the helix 6 point mutant could be reversed by excess LCAT.

The studies indicate that the low levels of HDL in patients with a mutation at residue 160 or 162 of apoA-I are the result of defective maturation of HDL due to impairment of the LCAT activity. The phenotype produced by mutations in residues 160 and 162 of apoA-I mimicked the phenotype observed in patients with classical LCAT deficiency (*9*) and may be overcome by an increase in the plasma concentration of LCAT.

EXPERIMENTAL PROCEDURES

Materials

Materials not mentioned in the experimental procedures have been obtained from sources described previously (*3*, *38*).

Methods

Generation of Adenoviruses Expressing the Wild-Type (WT) and Mutant ApoA-I Forms. The construction of recombinant adenoviruses carrying the genomic sequence for the WT apoA-I has been described previously (*28*). The adenoviruses expressing apoA-I[D102A/D103A], apoA-I[R160V/H162A], and apoA-I[Δ(144−165)] were generated in a similar way. Briefly, the fourth exon of the human apoA-I gene was amplified and mutagenized by polymerase chain reaction, using a set of specific mutagenic primers {AIMIV1-5 and AIMIV1-3 for apoA-I[D102A/D103A], AIMIV4-5 and AIMIV4-3 for apoA-I[R160V/H162A], and AIMIII3-5 and AIMIII3-3 for apoA-I[Δ(144−165)]} containing the mutation of interest and a set of flanking universal primers (AINOTF and AISALR) containing restriction sites *Not*I and *Sal*I. The sequences of the primers are given in Table 1. The pCA13AIgN vector, which contains a *Not*I site in intron 3 and a *Xho*I site at the 3′-end of the apoA-I gene, was used as a template in the amplification reactions (*28*, *39*). The DNA fragment containing the mutation of interest was digested with *Not*I and *Sal*I and subcloned into the *Not*I and *Xho*I sites of the pCA13AIgN vector, thus replacing the WT with the mutated exon 4 sequence. The pCA13-A-I plasmids, containing the D102A/D103A or R160V/H162A point mutations or the deletion of residues 144−165, along with a helper PJM17 adenovirus plasmid were used to generate recombinant adenoviruses as described previously (*28*, *38*).

Generation and Isolation of WT and Mutant ApoA-I Forms Using the Baculovirus Expression System. The generation of baculoviruses expressing WT apoA-I, the apoA-I[D102A/

Table 1: Oligonucleotide Sequences of Primers Used in PCR Amplifications

name	sequence	location of sequence
AIMIV1-5	5′-CAG CCC TAC CTG **GCC**[a] **GCC** TTC CAG AAG AA-3′	nucleotides 364−392 of apoA-I cDNA[b] (sense) (amino acids 98−107)
AIMIV1-3	5′-TT CTT CTG GAA **GGC** G**GC** CAG GTA GGG CTG-3′	nucleotides 392−364 (antisense) (amino acids 107−98)[c]
AIMIV4-5	5′-GAC GCG CTG **GTC** ACG **GCT** CTG GCC CC-3′	nucleotides 541−566 of apoA-I cDNA (sense) (amino acids 157−165)
AIMIV4-3	5′-GG GGC CAG **AGC** CGT **GAC** CAG CGC GTC-3′	nucleotides 566−541 of apoA-I cDNA (antisense) (amino acids 165−157)
AIMIII3-5	5′-GAG AAG CTG AGC CCA ... ...[d] TAC AGC GAC GAG CT-3′	nucleotides 487−501 and nucleotides 568−581 of apoA-I cDNA (sense) (amino acids 139−143 and amino acids 166−170)
AIMIII3-3	5′-AG CTC GTC GCT GTA ... ... TGG GCT CAG CTT CTC-3′	nucleotides 581−568 and nucleotides 501−487 of apoA-I cDNA (antisense) (amino acids 170−166 and amino acids 143−139)
AINOT F	5′-CCT CCG CGG ACA G**GC GGC CGC**[e] CAG GG-3′	nucleotides 886−911 of apoA-I genomic sequence[f] that contains a *Not*I site (sense), intron 3 of apoA-I gene
AISAL R	5′-A CAT **GTC GAC** CCC CTT TCA GGG CAC CTG GCC TTG-3′	ACAT, *Sal*I site, and nucleotides 1917−1894 of apoA-I genomic sequence (antisense), at 3′-end of apoA-I gene

[a] Mutagenized residues are marked in boldface type and are underlined. [b] Nucleotide number of the human apoA-I cDNA sequence (*71*), oligonucleotide position relative to the translation initiation ATG codon. [c] The amino acid positions refer to the mature plasma apoA-I sequence. [d] Deleted nucleotides are underlined. [e] The restriction enzyme recognition sites are marked in boldface type. [f] Nucleotide number of the human apoA-I genomic sequence (*39*), oligonucleotide position relative to the translation initiation ATG codon.

D103A] and apoA-I[R160V/H162A] point mutants, and the apoA-I[Δ(144−165)] deletion mutant was described previously (*3*, *40*). The expression and purification of recombinant WT and mutant apoA-I forms were performed as described previously (*1*, *3*).

Animal Studies, Plasma Lipids, ApoA-I, and ApoA-I mRNA Level Analyses. ApoA-I$^{-/-}$ (ApoA1^{tm1Unc}) C57BL/6J mice (*41*) were purchased from Jackson Laboratories (Bar Harbor, ME). The mice were maintained on a 12 h light/dark cycle and standard rodent chow. All procedures performed on the mice were in accordance with National Institutes of Health and institutional guidelines. ApoA-I$^{-/-}$ mice, 6−8 weeks of age, were injected via the tail vein with 1×10^9 pfu of recombinant adenovirus per animal and the animals sacrificed 4 days postinjection following a 4 h fast.

The concentrations of total cholesterol, free cholesterol, phospholipids, and triglycerides of plasma drawn 4 days postinfection were determined using the Total Cholesterol E, Free Cholesterol C, and Phospholipids B reagents (Wako Chemicals USA, Inc.) and INFINITY triglycerides reagent (ThermoDMA), respectively, according to the manufacturer's instructions. The concentration of cholesteryl esters was determined by subtracting the concentration of free cholesterol from the concentration of total cholesterol. Plasma apoA-I levels and hepatic human apoA-I mRNA levels were determined as described previously (*1*, *3*).

For FPLC analysis of plasma, 17 μL of plasma obtained from mice infected with adenovirus-expressing WT or mutant apoA-I forms was loaded onto a Sepharose 6 PC column (Amersham Biosciences) in a SMART micro FPLC system (Amersham Biosciences) and eluted with PBS. A total of 25 fractions 50 μL in volume each were collected for further analysis. The concentration of lipids and apoA-I in the FPLC fractions was determined as described above.

Fractionation of Plasma by Density Gradient Ultracentrifugation and Electron Microscopy Analysis of the ApoA-I-Containing Fractions. For this analysis, 300 μL of plasma obtained from adenovirus-infected mice was diluted with saline to a total volume of 0.5 mL. The mixture was adjusted to a density of 1.23 g/mL with KBr and overlayed with 1 mL of a KBr solution with a *d* of 1.21 g/mL, 2.5 mL of a KBr solution with a *d* of 1.063 g/mL, 0.5 mL of a KBr solution with a *d* of 1.019 g/mL, and 0.5 mL of normal saline. The mixture was centrifuged for 22 h in a SW55 rotor at 30 000 rpm. Following ultracentrifugation, 0.5 mL fractions were collected from the top and analyzed as described previously (*1*).

For electron microscopy analysis, the fractions that float in the HDL region were treated and photographed as described previously (*1*).

Nondenaturing Two-Dimensional Electrophoresis. The distribution of HDL subfractions in plasma was analyzed by two-dimensional electrophoresis as described previously (*42*) with some modifications. Briefly, in the first dimension, 2 μL of plasma sample was separated by electrophoresis at 4 °C in a 0.75% agarose gel using a 50 mM barbital buffer (pH 8.6, Sigma, St. Louis, MO) until the bromophenol blue marker had migrated 5.5 cm. Agarose gel strips containing the separated lipoproteins were then transferred to a 4 to 20% polyacrylamide gradient gel. Separation in the second dimension was performed at 90 V for 2−3 h at 4 °C. The separated proteins were transferred to a nitrocellulose membrane, and human apoA-I was detected by probing the membrane with a goat polyclonal anti-human apoA-I antibody (Chemicon International), and mouse apoE was detected by probing the membrane with a goat polyclonal anti-mouse apoE antibody (Santa Cruz Biotechnology Inc., Santa Cruz, CA).

Production, Purification, and Activation of LCAT by WT and Mutant ApoA-I Forms. LCAT was purified as described (*38*, *43*, *44*) from the culture medium of human HTB13 cells infected with an adenovirus expressing the human LCAT cDNA (*45*), which was a generous gift of S. Santamarina-Fojo. For LCAT analysis, the reconstituted HDL (rHDL)

particles, used as the substrate, contained cholesterol and [^{14}C]cholesterol ([4-^{14}C]cholesterol, 0.04 mCi/mL, specific activity of 45 mCi/mmol; Perkin-Elmer Life Sciences, Inc.), β-oleoyl-γ-palmitoyl-L-α-phosphatidylcholine (POPC), and apoA-I and were prepared by the sodium cholate dialysis method as described previously (*2*, *46*). The reactions were carried out as described previously (*2*, *38*). The cholesterol esterification rate was expressed as nanomoles of cholesteryl ester formed per hour. To calculate the apparent V_{max} and K_m, the rate of cholesteryl ester formation was plotted versus the concentration of apoA-I. The data were fitted to Michaelis−Menten kinetics, using Prism (GraphPad Software, Inc.). Because of the low catalytic activity of the apoA-I[R160V/H162A] and apoA-I[Δ(144−165)] mutants, their $K_{max-app}$ and $V_{max-app}$ values were obtained as described previously (*2*, *38*) for the WT apoA-I using a 25-fold higher enzyme concentration. To compare the kinetic parameters of the WT apoA-I and the apoA-I[R160V/H162A] and apoA-I[Δ(144−165)] mutants, the $V_{max-app}$ values of the two mutants were normalized by dividing the experimentally obtained $V_{max-app}$ by 25.

RESULTS

LCAT Activation in Vitro. For LCAT activation, WT and the three mutant apoA-I forms were produced using the baculovirus system and were subsequently used for the generation of discoidal rHDL particles as described previously (*27*, *38*). The LCAT activity was assayed as the rate of production of labeled cholesteryl esters from the ^{14}C-labeled rHDL particles. The cholesterol content of the rHDL particles containing the WT and the three mutant apoA-I forms was comparable (data not shown). The esterification of the cholesterol of the rHDL particles containing the helix 6 point mutant (helix 6P) apoA-I[R160A/H162A] and the helix 6 deletion mutant (helix 6Δ) apoA-I[Δ144−165] in vitro was very low and could be overcome with excess LCAT. It was found that a 25-fold increase in enzyme concentration resulted in initial velocities of esterification comparable to those obtained with WT apoA-I and a 1-fold enzyme concentration. Using the 25-fold excess of enzyme concentration, the K_{m-app} and $V_{max-app}$ values of the mutants were calculated and compared to those of WT apoA-I as described in Experimental Procedures (Figure 1). Both mutants had greatly reduced $V_{max-app}$ values and increased K_{m-app} values compared to those of WT apoA-I (Figure 1). The apparent catalytic efficiencies ($V_{max-app}/K_{m-app}$) of the enzyme using rHDL particles containing the helix 6P and helix 6Δ mutants were estimated to be ∼0.7 and 0.4% of the WT control, respectively, whereas that of the helix 4 point mutant (helix 4P) apoA-I[D102A/D103A] was 50% of the WT control (Figure 1). The low catalytic efficiencies of the helix 6P and helix 6Δ mutants are comparable with previously published values (*22*, *24*, *47*−*49*).

Plasma Lipid, ApoA-I, and Hepatic ApoA-I mRNA Levels following Adenovirus Infection. Analysis of plasma lipids and apoA-I levels and hepatic apoA-I mRNA levels 4 days postinfection showed that apoA-I$^{-/-}$ mice infected with adenoviruses expressing the WT apoA-I and the helix 4P mutant had normal levels of total, free, and esterified cholesterol and similar CE/TC ratios compared with C57BL/6 mice, whereas apoA-I$^{-/-}$ mice infected with adenoviruses expressing the helix 6P and helix 6Δ mutants and apoA-I$^{-/-}$ mice infected with the control adenovirus expressing the green fluorescence protein (apoA-I$^{-/-}$ GFP) had reduced levels of total, free, and esterified cholesterol and a decreased CE/TC ratio (Table 2). The plasma apoA-I levels were high in mice expressing WT apoA-I, normal in mice expressing the helix 4P and helix 6P mutants, and diminished in mice expressing the helix 6Δ mutant (Table 2). The phospholipid levels were normal in mice expressing the WT apoA-I and the helix 4P and helix 6P mutants, but were greatly reduced in mice expressing the helix 6Δ mutant and the control mice that express GFP (Table 2). The levels of plasma triglycerides in mice expressing the WT or mutant apoA-I forms were moderately increased as compared to those for apoA-I$^{-/-}$ GFP and C57BL/6 mice (Table 2). The differences in plasma lipid and apoA-I levels may not reflect differences in apoA-I expression, since the relative amounts of apoA-I mRNA were comparable (Table 2). However, we cannot exclude the possibility of differences in translation efficiencies or in vivo secretion between the WT and mutant apoA-I forms.

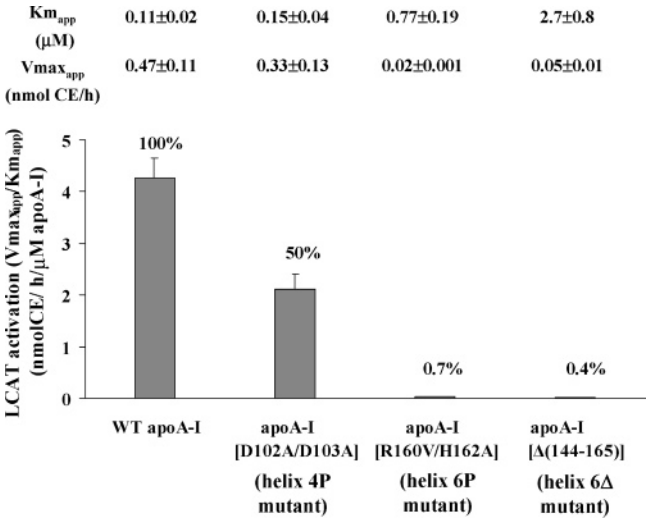

FIGURE 1: Activation of LCAT by rHDL containing WT or mutant apoA-I forms. Experiments were performed as described in Experimental Procedures using the indicated WT and mutant apoA-I forms. Values are the means ± the standard deviation from three independent experiments performed in duplicate.

FPLC Profiles of Plasma Isolated from Mice Infected with Adenoviruses Expressing the WT and the Three Mutant ApoA-I Forms. FPLC analysis of plasma from apoA-I$^{-/-}$ mice infected with recombinant adenoviruses expressing either the WT apoA-I or the helix 4P mutant 4 days postinfection showed that apoA-I, cholesterol, and phospholipids were distributed predominantly in the HDL_2 and HDL_3 region (Figure 2A−C). The cholesteryl ester profiles were identical to those of total cholesterol (data not shown). Small amounts of apoA-I and cholesterol and barely detectable levels of phospholipids were also found in the HDL_2 and HDL_3 region in mice infected with the adenovirus expressing the helix 6Δ mutant (Figure 2A−C). The HDL cholesterol levels in these mice were comparable to the HDL cholesterol levels of mice infected with the control adenovirus expressing the GFP (Figure 2B). In all mice infected with adenoviruses, the triglycerides were distributed in the VLDL region (Figure 2D).

A different apoA-I, cholesterol, and phospholipid FPLC profile was observed in mice infected with the adenovirus expressing the helix 6P mutant. In these mice, high levels

Table 2: Comparison of Plasma Lipids and ApoA-I Levels and Hepatic mRNA Levels of ApoA-I$^{-/-}$ Mice 4 Days Postinfection with Recombinant Adenoviruses Expressing the WT ApoA-I or ApoA-I Mutants or the Control Protein GFP[a]

	human apoA-I (mg/dL)	TC (mg/dL)	FC (mg/dL)	CE (mg/dL)	CE/TC (mg/dL)	PL (mg/dL)	TG (mg/dL)	relative hepatic human apoA-I mRNA (%)
WT apoA-I	432 ± 84	101 ± 15	31 ± 16	70 ± 19	0.69 ± 0.08	262 ± 48	101 ± 19	100
apoA-I[D102A/D103A] (helix 4P mutant)	98 ± 24	95 ± 18	24 ± 2	72 ± 19	0.74 ± 0.05	138 ± 30	63 ± 14	73 ± 8
apoA-I[R160V/H162A] (helix 6P mutant)	140 ± 16	57 ± 28	31 ± 15	26 ± 13	0.45 ± 0.06	179 ± 74	73 ± 10	113 ± 29
apoA-I[Δ(144−165)] (helix 6Δ mutant)	33 ± 6	44 ± 14	22 ± 7	22 ± 9	0.50 ± 0.07	63 ± 16	68 ± 16	84 ± 7
apoA-I$^{-/-}$ GFP	−	35 ± 6	17 ± 7	18 ± 1	0.52 ± 0.11	81 ± 14	42 ± 7	−
C57Bl/6	112 ± 10[b] (mouse plasma apoA-I)	95 ± 8	27 ± 5	68 ± 3	0.72 ± 0.02	256 ± 10	43 ± 6	−

[a] Parameters for C57Bl/6 mice are also provided. Values are means ± the standard deviation ($n = 4-6$). [b] The value for mouse plasma apoA-I was obtained from ref *72*.

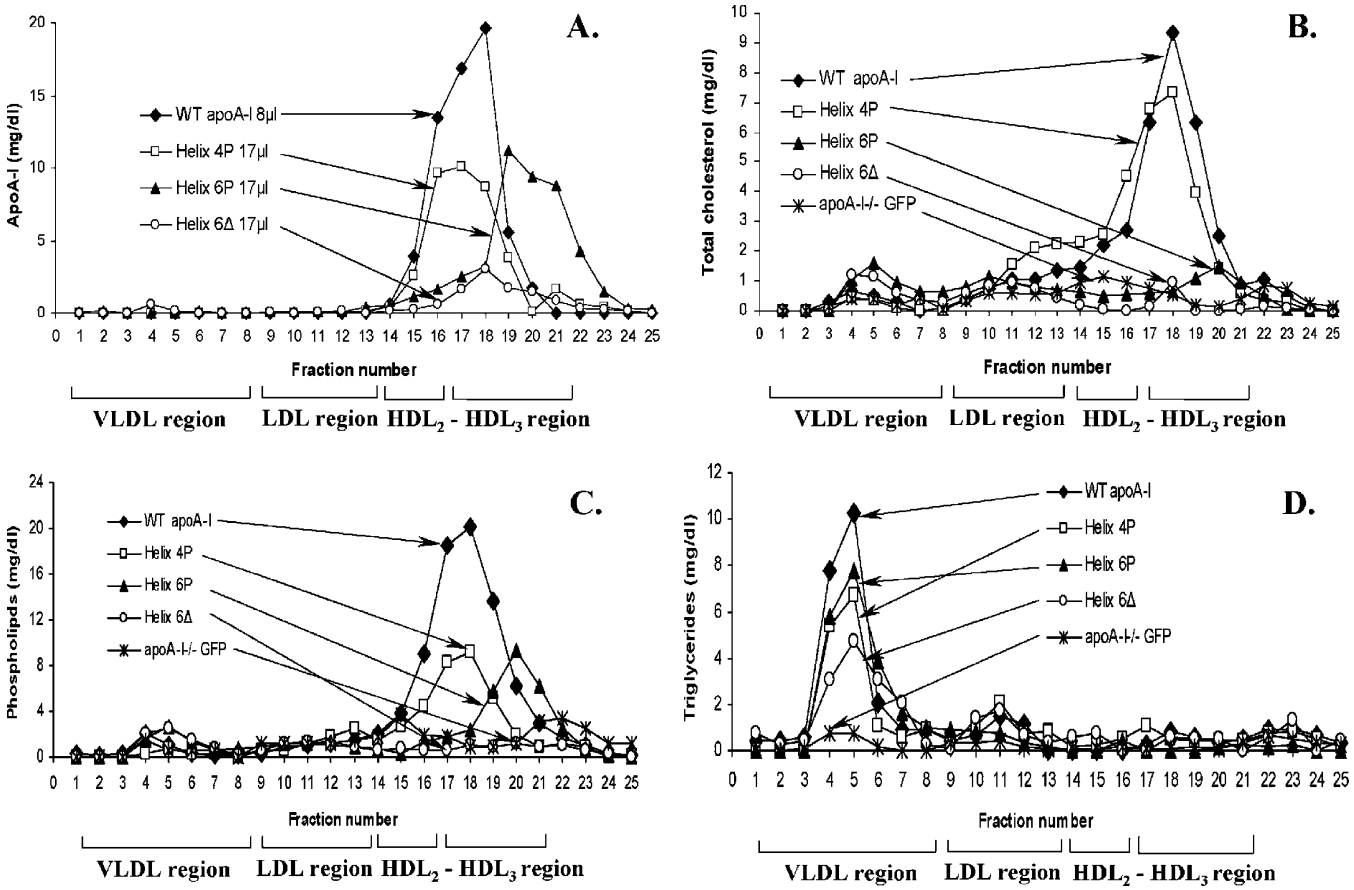

FIGURE 2: FPLC profiles of apoA-I, total cholesterol, phospholipids, and triglycerides in plasma of apoA-I$^{-/-}$ mice expressing the WT apoA-I, the helix 4P (apoA-I[D102A/D103A]), helix 6P (apoA-I[R160V/H162A]), or helix 6Δ {apoA-I[Δ(144−165)]} mutant, or the control protein GFP. Plasma samples were obtained from mice infected with 1×10^9 pfu of the recombinant adenoviruses expressing the WT or mutant forms of apoA-I or the control protein GFP 4 days postinfection. The samples were fractionated by FPLC, and then the apoA-I (A), total cholesterol (B), phospholipid (C), and triglyceride (D) levels of each FPLC fraction were determined as described in Experimental Procedures.

of apoA-I and phospholipids and lower levels of cholesterol were found in the HDL_3 region (Figure 2A−C). The cholesteryl ester profile was identical to that of the total cholesterol (data not shown).

Effect of the ApoA-I Point Mutations in Helices 4 (apoA-I[D102A/D103A]) and 6 (apoA-I[R160A/H162A]) and Deletion of Helix 6 (apoA-I[Δ144−165]) on the Distribution of ApoA-I in Different Lipoproteins and the Size and Shape of HDL. Analysis of the distribution of apoA-I following density gradient ultracentrifugation of plasma showed that in mice infected with adenoviruses expressing the WT apoA-I and the helix 4P mutant, apoA-I was distributed in the HDL_2 and HDL_3 region (Figure 3A). In mice expressing the WT apoA-I, the peak concentration of apoA-I was in the HDL_2 region, and in mice expressing the helix 4P mutant, apoA-I was equally distributed in the HDL_2 and HDL_3 region (Figure 3A). Consistent with the FPLC data (Figure 2A) in mice infected with the helix 6P mutant, the peak concentration of apoA-I was in the HDL_3 region (Figure 3A). Finally, in mice infected with the adenovirus expressing the helix 6Δ mutant, apoA-I was equally distributed in HDL_2 and HDL_3 (Figure 3A), whereas a substantial portion of HDL was also found

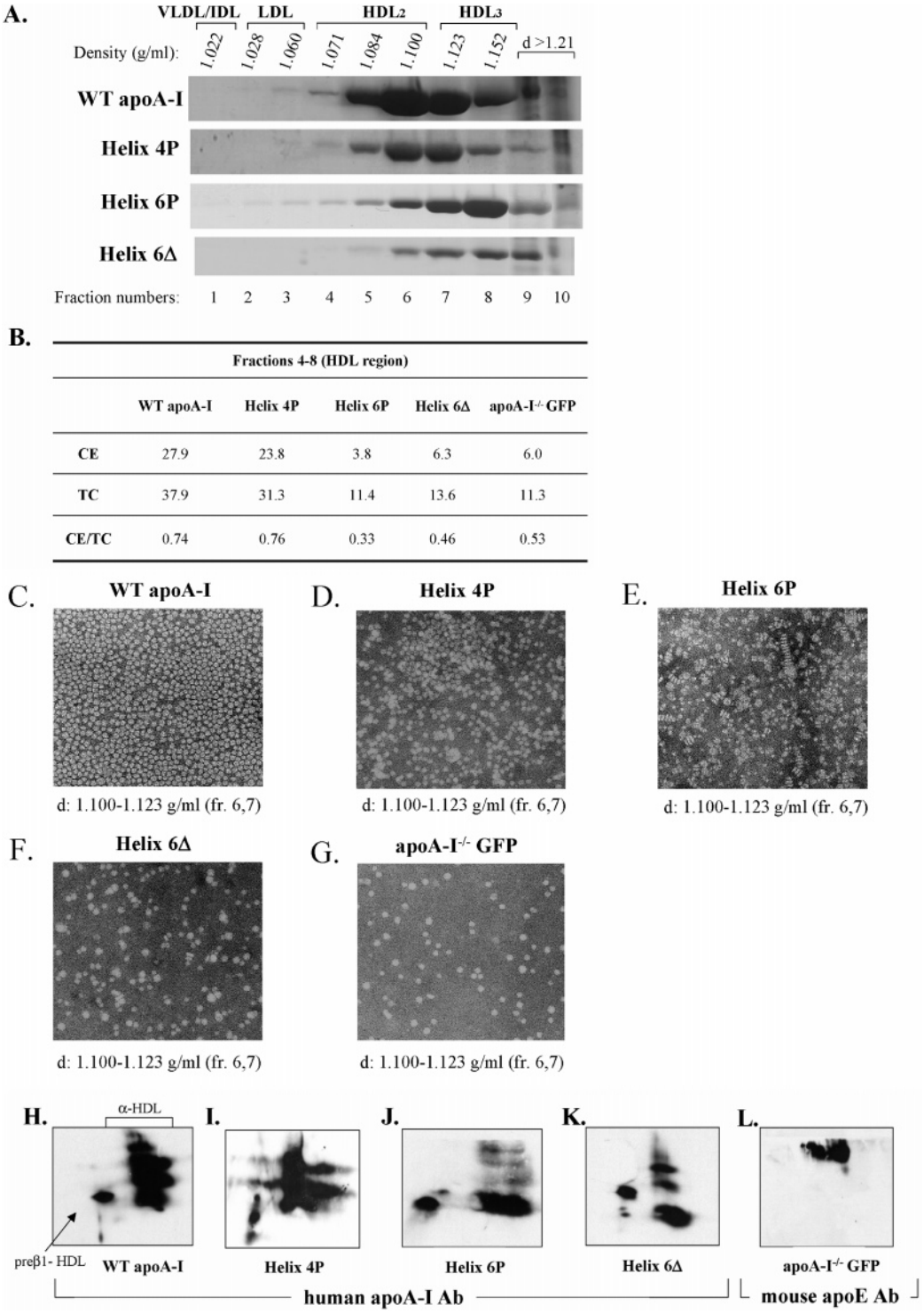

FIGURE 3: Analyses of plasma of apoA-I$^{-/-}$ mice expressing the WT apoA-I, the helix 4P (apoA-I[D102A/D103A]), helix 6P (apoA-I[R160V/H162A]), or helix 6Δ {apoA-I[Δ(144−165)]} mutant, or the control protein GFP. (A) SDS−PAGE analysis of density gradient ultracentrifugation fractions of plasma of apoA-I$^{-/-}$ mice expressing the WT or mutant apoA-I forms. Fractionation of plasma was performed as described in Experimental Procedures. The densities of the fractions are indicated at the top. (B) CE/TC ratio from a pool of lipoprotein fractions that correspond to the HDL region (fractions 4−8). (C−G) Electron microscopy pictures of HDL fractions obtained from apoA-I$^{-/-}$ mice expressing the WT apoA-I (C), the helix 4P (D), helix 6P (E), or helix 6Δ (F) mutant, or the control protein GFP (G) following density gradient ultracentrifugation of plasma. The densities of the fractions used are given at the bottom. The photomicrographs were taken at 75000× magnification and enlarged three times. (H−L) Analysis of plasma obtained from mice expressing the WT apoA-I (H), the helix 4P (I), helix 6P (J), or helix 6Δ (K) mutant, or the control GFP protein (L) following two-dimensional gel electrophoresis and Western blotting using anti-human apoA-I antibody (H−K) or anti-mouse apoE antibody (L), as described in Experimental Procedures.

in the $d > 1.21$ g/mL fraction that was shown by electron microscopy to lack any lipoprotein particles (data not shown).

Analysis of the distribution of total cholesterol, cholesteryl ester, free cholesterol, triglycerides, and phospholipids following density gradient ultracentrifugation of plasma essentially confirmed the distribution of these lipids to different lipoprotein fractions that were obtained by FPLC fractionation (data not shown). The cholesteryl ester (CE) to total

Table 3: Comparison of Plasma Lipids and ApoA-I Levels of ApoA-I$^{-/-}$ Mice 4 Days Postinfection with Recombinant Adenoviruses Coexpressing a Combination of WT or Mutant ApoA-I Forms or GFP and LCAT[a]

	apoA-I (mg/dL)	TC (mg/dL)	FC (mg/dL)	CE (mg/dL)	CE/TC (mg/dL)	PL (mg/dL)	TG (mg/dL)	relative hepatic apoA-I mRNA[b] (%)
WT apoA-I	254 ± 88	214 ± 28	44 ± 5	169 ± 23	0.79 ± 0.02	244 ± 39	65 ± 3	68 ± 20
apoA-I[R160V/H162A] (helix 6P mutant)	463 ± 25	461 ± 59	116 ± 26	345 ± 33	0.74 ± 0.03	571 ± 43	166 ± 44	91 ± 28
apoA-I[Δ(144−165)] (helix 6Δ mutant)	45 ± 3	144 ± 4	31 ± 1	113 ± 6	0.79 ± 0.01	170 ± 9	62 ± 7	44 ± 9
apoA-I$^{-/-}$ GFP	−	116 ± 40	29 ± 9	87 ± 31	0.75 ± 0.01	139 ± 34	46 ± 2	−

[a] Values are means ± the standard deviation ($n = 4$). [b] The value of hepatic apoA-I mRNA levels was taken to be 100% in mice infected with adenoviruses expressing WT apoA-I (but not LCAT) (Table 2).

cholesterol (TC) ratio was calculated in fractions 4−8 that correspond to the HDL region (Figure 3A). This analysis showed that the CE/TC ratio in mice infected with the helix 6P and helix 6Δ mutants was comparable to or lower than that of the mice infected with the GFP-expressing adenovirus and was greatly reduced as compared to the CE/TC ratio of mice infected with adenoviruses expressing the WT apoA-I or the helix 4P mutant (Figure 3B). As suggested previously (*50*), the low CE/TC ratio indicates defective esterification of HDL in vivo in mice infected with the adenoviruses expressing the helix 6P and helix 6Δ mutants of apoA-I. Similar information for the CE/TC ratio of the HDL region was obtained by fractionation of plasma by FPLC (data not shown).

Analysis by electron microscopy of HDL fractions 6 and 7 (density, 1.100−1.123 g/mL), obtained by density gradient ultracentrifugation (Figure 3A), showed that both the WT apoA-I and the helix 4P mutant promoted the formation of spherical HDL particles (Figure 3C,D), whereas the helix 6P mutant promoted predominantly the formation of discoidal HDL particles (Figure 3E). In contrast, the helix 6Δ mutant promoted the formation of few spherical particles (Figure 3F) similar to those seen in control mice infected with the adenovirus-expressing GFP (Figure 3G). Two-dimensional gel electrophoresis of plasma showed that both the WT apoA-I and the helix 4P mutant formed α-HDL particles and small amounts of preβ1-HDL particles (Figure 3H,I), whereas both the helix 6P mutant and the helix 6Δ mutant had an increased ratio of preβ1 to α-HDL particles and reduced the population of the larger α-HDL particles (Figure 3J,K). This reduction in the larger α-HDL particles was more pronounced in the case of the helix 6P mutant.

In the analyses shown in Figure 3H−K, apoA-I-containing HDL particles were detected on the membrane blots with anti-human apoA-I antibodies. When blots were treated with antibodies to mouse apoE, apoE containing particles of fast electrophoretic mobility and larger size were detected in the plasma of apoA-I$^{-/-}$ mice infected with the control GFP-expressing adenovirus (Figure 3L), but not in the plasma of mice infected with adenoviruses expressing the WT or mutant apoA-I forms (data not shown).

In Vivo Effect of LCAT on Plasma Lipids, FPLC Profiles, the Distribution of HDL in Different Densities, and the Size and Shape of HDL in Mice Infected with Adenoviruses Expressing WT or Helix 6P or Helix 6Δ Mutant ApoA-I Forms and Human LCAT. To assess how apoA-I mutations affect the biogenesis of HDL, apoA-I$^{-/-}$ mice were coinfected with a mixture of adenoviruses expressing WT or mutant apoA-I forms (1×10^9 pfu) along with human LCAT (1×10^9 pfu). This treatment increased more than 2-fold the levels of total cholesterol and cholesteryl esters in mice infected with the adenovirus expressing the WT apoA-I, without altering the CE/TC ratio (Tables 2 and 3). This treatment did not affect the FPLC profile of apoA-I, but shifted the FPLC HDL cholesterol profile to the HDL_2 region (Figure 4A,D). The reduction in plasma apoA-I levels can be attributed to the decreased levels of hepatic apoA-I mRNA (Tables 2 and 3). A similar increase in the HDL_2 cholesterol level was observed in apoA-I$^{-/-}$ mice infected with a mixture of adenoviruses expressing GFP and human LCAT (Figure 4G).

The LCAT coinfection had a dramatic effect in mice infected with the helix 6P mutant. This treatment increased 3.3-, 8-, and 13-fold the apoA-I, the total cholesterol, and the esterified cholesterol levels, respectively, and normalized the CE/TC ratio of HDL (Tables 2 and 3). The relative expression levels of hepatic apoA-I mRNA with or without LCAT coinfection were comparable (Tables 2 and 3). All the increase in the cholesterol level could be attributed to the increase in the plasma apoA-I and HDL level (Figure 4B,E). The LCAT coinfection also increased approximately 4-fold the plasma-free cholesterol, 3-fold the plasma phospholipid, and 2-fold the plasma triglyceride levels (Tables 2 and 3). The increase in the plasma triglyceride level most likely is associated with the presence of apoA-I in the VLDL/IDL fraction (Figure 5D) (*27*, *38*). In mice coinfected with adenoviruses expressing LCAT and the helix 6Δ mutant or the control GFP, lipid parameters (with the exception of those of free cholesterol and triglycerides) increased 3−5-fold and the CE/TC ratio of HDL was normalized (Tables 2 and 3). The LCAT coinfection also caused an increase in plasma apoA-I and HDL levels in mice infected with the adenovirus-expressing helix 6Δ mutant (Tables 2 and 3 and Figure 4C,F). The increase in plasma apoA-I level corrected for hepatic apoA-I mRNA levels was 2.5-fold (Tables 2 and 3). The LCAT coinfection shifted the FPLC HDL cholesterol and apoA-I profile toward the HDL_2 region (Figure 4C,F).

Useful information was obtained by comparison of the relative distribution of apoA-I, apoE, and apoA-IV in the plasma of mice infected with adenoviruses expressing WT and mutant apoA-I forms or the control GFP with or without concomitant infection with adenovirus expressing LCAT. In mice expressing the helix 6Δ mutant, the LCAT treatment increased the concentration of apoE in the HDL_2 and LDL region and also shifted and increased the concentration of apoA-IV in the HDL_2 and HDL_3 region (Figure 5E,F). Similar changes in concentration and shifts toward lower densities of apoE and apoA-IV following treatment with LCAT were observed in mice infected with the adenovirus expressing WT apoA-I or the control adenovirus expressing

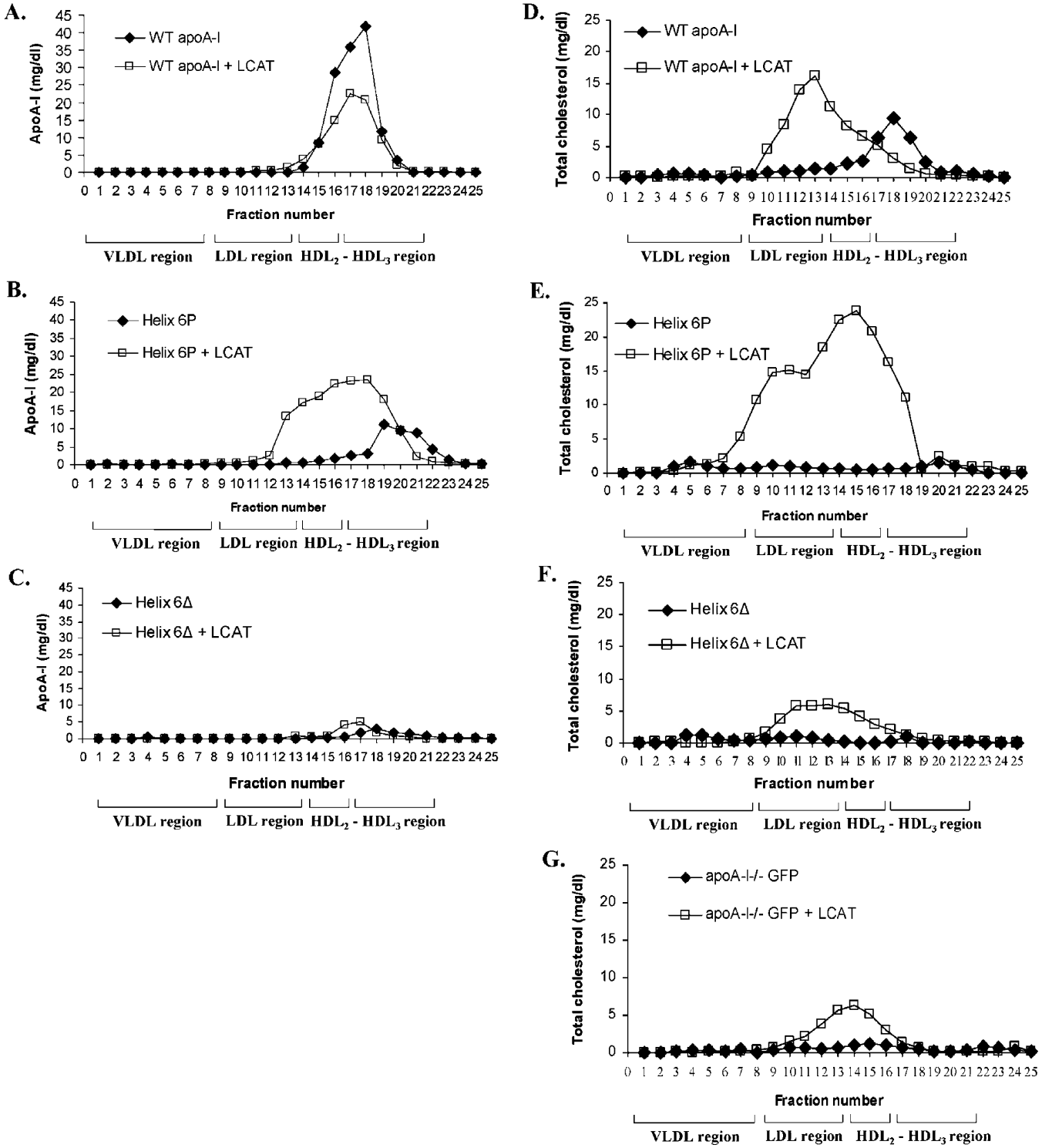

FIGURE 4: FPLC profiles of apoA-I and total cholesterol in plasma of apoA-I$^{-/-}$ mice expressing the WT apoA-I, the helix 6P mutant (apoA-I[R160V/H162A]), or the helix 6Δ mutant {apoA-I[Δ(144−165)]} as well as FPLC profile of total cholesterol in plasma of apoA-I$^{-/-}$ mice expressing the control protein GFP, alone or in combination with human LCAT. Plasma samples were obtained from mice infected with 1×10^9 pfu of the recombinant adenoviruses expressing the WT or mutant forms of apoA-I alone or in combination with 1×10^9 pfu of an adenovirus expressing the human LCAT 4 days postinfection. The samples were fractionated by FPLC, and then the apoA-I (A−C) and total cholesterol (D−G) levels of each FPLC fraction were determined as described in Experimental Procedures.

GFP (Figure 5A,B,G,H). The shifts in the distribution of apoE and apoA-I that were caused by LCAT treatment seen in Figure 5A,B,E−H parallel the shifts in cholesterol distribution observed in Figure 4D,F,G. The shift in the cholesterol peak toward the LDL region may represent partial esterification of LDL cholesterol, which as reported previously can be promoted by apoE (*51*, *52*). In addition, it may reflect the formation of apoE-containing HDL particles. The LCAT treatment of mice expressing the helix 6P mutant shifted the bulk of apoA-I from HDL_3 to the HDL_2 and LDL region, while a small amount of apoA-I was also found in the VLDL and IDL region (Figure 5C,D). Only small amounts of apoE and apoA-IV were detected in the VLDL and LDL region and HDL_2 region, respectively, and their

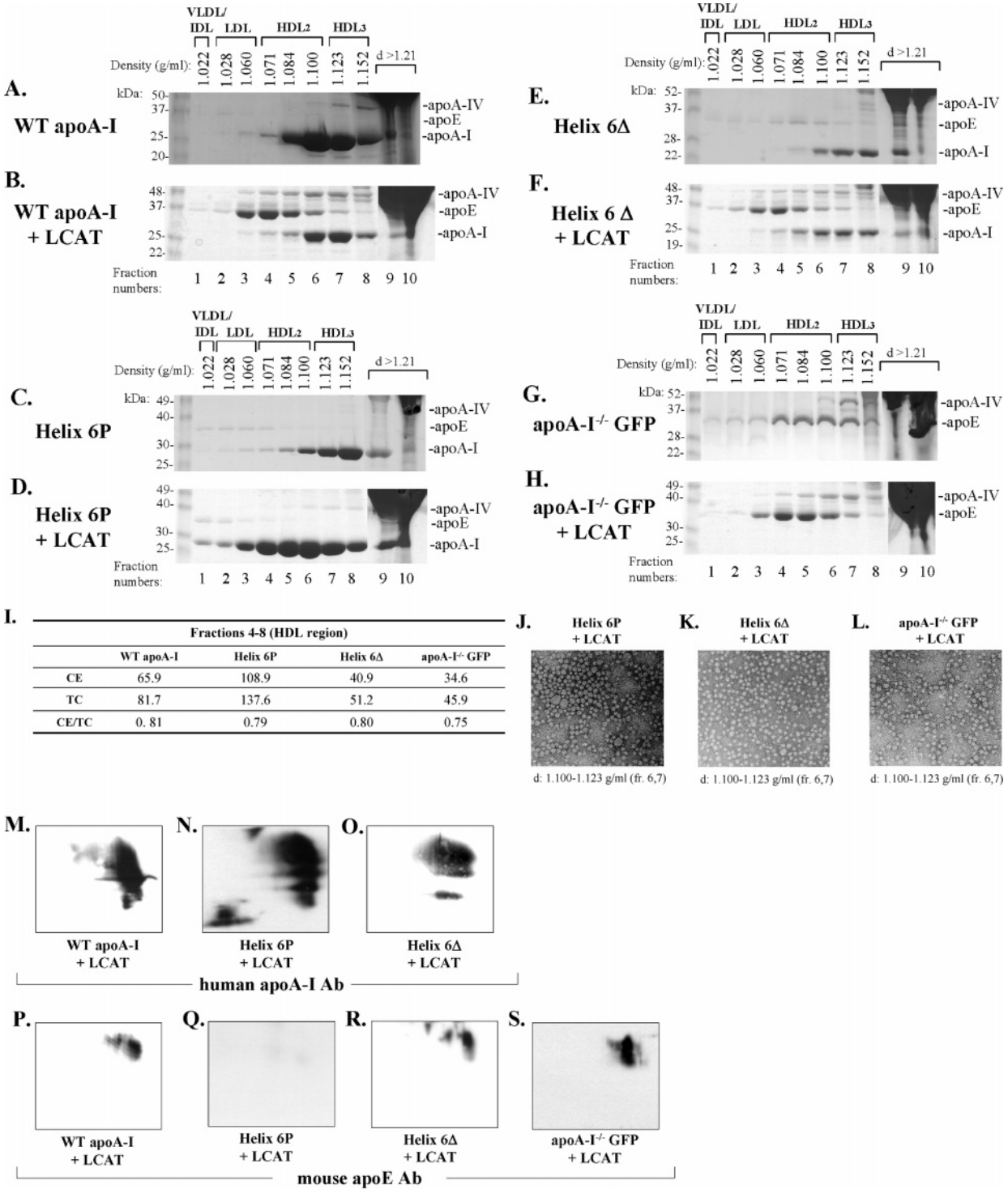

I.

Fractions 4-8 (HDL region)				
	WT apoA-I	Helix 6P	Helix 6Δ	apoA-I-/- GFP
CE	65.9	108.9	40.9	34.6
TC	81.7	137.6	51.2	45.9
CE/TC	0. 81	0.79	0.80	0.75

FIGURE 5: Analyses of plasma of apoA-I$^{-/-}$ mice expressing the WT apoA-I, the helix 6P (apoA-I[R160V/H162A]) or helix 6Δ {apoA-I[Δ(144−165)]} mutant, or the control protein GFP alone or in combination with human LCAT. (A−H) Comparison of the SDS−PAGE profiles of fractions obtained by density gradient ultracentrifugation analysis of plasma of apoA-I$^{-/-}$ mice expressing the WT or mutant apoA-I forms alone or in combination with the human LCAT. Fractionation of plasma and SDS−PAGE analysis was performed as described in Experimental Procedures. Panels A, C, E, and G correspond to plasma samples obtained from mice expressing the WT apoA-I (A), the helix 6P (C) or helix 6Δ (E) mutant, or the control protein GFP (G) alone. Panels B, D, F, and H correspond to plasma samples obtained from mice expressing the WT apoA-I (B), the helix 6P (D) or helix 6Δ (F) mutant, or the control protein GFP (H) in combination with human LCAT. The densities of the fractions are indicated at the top. (I) CE/TC ratio from a pool of lipoprotein fractions that correspond to the HDL region (fractions 4−8). (J−L) Electron microscopy pictures of HDL fractions obtained from apoA-I$^{-/-}$ mice expressing the helix 6P (J) and helix 6Δ (K) mutants along with human LCAT or the control protein GFP (L) along with human LCAT, following density gradient ultracentrifugation of plasma. The densities of the fractions are indicated at the bottom of each panel. The photomicrographs were taken at 75000× magnification and enlarged three times. (M−S) Analysis of plasma obtained from mice expressing the WT apoA-I (M and P), the helix 6P (N and Q), or helix 6Δ (O and R) mutant, or the control GFP protein (S) together with human LCAT following two-dimensional gel electrophoresis and Western blotting using anti-human apoA-I antibody (M−O) or anti-mouse apoE antibody (P−S), as described in Experimental Procedures.

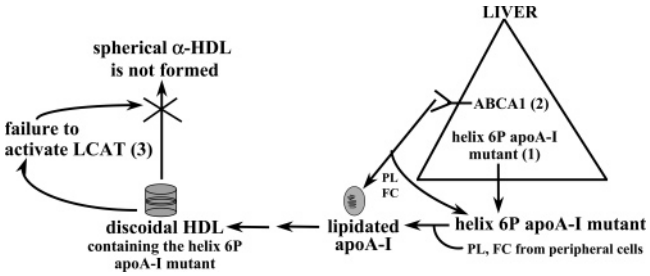

FIGURE 6: Schematic representation of the early steps in the biogenesis of HDL. Numbers 1−3 indicate different steps in the biogenesis of HDL. When step 1 or 2 is inhibited, we observe only formation of preβ1-HDL (*1*, *4*, *9*, *14*). This figure indicates that when step 3 is inhibited or the activity of LCAT is rate-limiting we observe accumulation of discoidal HDL particles.

concentration and the distribution to different densities did not change following treatment with LCAT (Figure 5C,D). The LCAT treatment also normalized the CE/TC ratio of HDL in mice infected with adenoviruses expressing the helix 6P mutant and helix 6Δ mutant as well as in mice infected with the GFP-expressing adenovirus (Figure 5I). It also promoted the formation of only spherical particles in mice expressing the helix 6P and helix 6Δ apoA-I mutants or the GFP (Figure 5J−L).

Two-dimensional electrophoresis of plasma showed that following LCAT coinfection the WT apoA-I, the helix 6P mutant, and the helix 6Δ mutant produced large α-HDL particles (compare Figure 5M−O with Figure 3H,J,K). In the case of WT apoA-I and the helix 6Δ mutant, the LCAT treatment eliminated completely the preβ1-HDL particles (Figure 5M,O). When duplicate blots corresponding to those shown in Figure 5M−O were treated with antibodies to mouse apoE, apoE-containing lipoproteins with fast electrophoretic mobility and larger size were detected in the plasma of apoA-I-deficient mice infected with adenoviruses expressing the WT apoA-I or the helix 6Δ mutant (Figure 5P,R), but not in mice expressing the helix 6P mutant (Figure 5Q). ApoE-containing particles were also detected in the plasma of mice coinfected with adenoviruses expressing LCAT and the control protein GFP (Figure 5S).

Figure 6 is a schematic representation depicting the effect of apoA-I mutations with reduced capacity to activate LCAT, such as the helix 6P mutant, on the biogenesis of spherical HDL.

DISCUSSION

Effect of ApoA-I Mutations on Different Steps in the Pathway of Biogenesis of HDL. ApoA-I bound to lipids is the principal physiological activator of LCAT (*53*). It has been shown that particles containing one molecule of apoA-I complexed with small amounts of phospholipids and cholesterol are efficient substrates for LCAT (*54*).

The capacity of apoA-I mutations to activate LCAT has been studied extensively in vitro and, in a few instances, in vivo (*2*, *18*−*28*, *31*−*37*, *47*−*49*, *55*−*63*).

All these studies invariably suggested that although several domains of apolipoprotein A-I may contribute to the activation of LCAT, helix 6 of apoA-I, which contains residues 143−164, is essential for this process.

The hydrophobic−hydrophilic interface of helix 6 of apoA-I contains a cluster of three conserved arginine residues (R149, R153, and R160), which were suggested to create a positive electrostatic potential around apoA-I (*48*). Mutations in these residues reduced drastically the ability of rHDL particles containing these apoA-I mutants to activate LCAT in vitro. On the basis of the "belt" model for discoidal rHDL, it was suggested that residues R149, R153, and R160 are located on the hydrophilic face of the apoA-I helices and do not form intramolecular salt bridges in the antiparallel apoA-I dimer that covers the fatty acyl chain of the discoidal particle (*8*, *48*, *64*). This arrangement could allow in principle these apoA-I residues to form salt bridges or hydrogen bonds with appropriate residues of LCAT and thus contribute to LCAT activation.

LCAT activation was also severely impaired in vitro by the naturally occurring mutations R151C and H162Q (*24*, *62*, *63*). These residues are found in the hydrophilic face of the helix, and it was proposed, on the basis of the belt model for discoidal HDL, that residue 162 participates in interhelical interactions with D103 in the apoA-I dimer (*8*, *64*).

On the basis of the background information discussed above and our previous work (*3*), in the current study we have focused on the impact of two sets of point mutations near the kinks on helices 4 and 6 and a deletion of helix 6 on the activation of LCAT.

ApoA-I mutants offer a valuable tool for dissecting the molecular events which lead to the biogenesis of HDL and possibly for understanding the types of molecular interactions between apoA-I and LCAT which lead to the activation of the enzyme.

It has been established that the interactions of lipid-free apoA-I with ABCA1 are essential for the biogenesis of HDL (*1*, *65*, *66*). Mutations in the ABCA1 transporter that affect its functional interactions with lipid-free apoA-I prevent the formation of either spherical or discoidal HDL (*9*). We have also shown that carboxy-terminal deletions which eliminate residues 220−231 of apoA-I interact poorly with ABCA1 and fail to form either discoidal or spherical HDL (*1*, *4*). Following the initial lipidation of apoA-I via ABCA1 (*66*), the next crucial step in the biogenesis of HDL is the conversion of discoidal to spherical HDL (Figure 6). It is well established that structural mutations in LCAT which affect the catalytic functions of the enzyme are associated with the classical form of LCAT deficiency which is characterized by the accumulation in plasma of discoidal HDL particles (*16*). This phenotype clearly implies that deficiency in LCAT activity, due to critical mutations in the enzyme or mutations in the activator apoA-I, permits the early steps in HDL biogenesis to proceed, but the discoidal HDL that is produced cannot be converted to spherical particles (Figure 6).

Identification of Point Mutations in ApoA-I that Inhibit LCAT in Vivo and Generate a Phenotype that Mimics the Classical LCAT Deficiency. To dissect the effect of different apoA-I mutations on the biogenesis and/or remodeling of HDL, we have used various HDL parameters, including the HDL cholesterol peak following FPLC fractionation of plasma, the formation of discoidal or spherical HDL as determined by electron microscopy, and the relative abundance of preβ1 and α-HDL particles. Two other in vivo parameters were important. The first was the in vivo capacity of the mouse LCAT to esterify the HDL cholesterol in mice expressing mutant apoA-I forms as determined by the CE/

TC ratio of the HDL fraction. The second was the restoration of the CE/TC ratio and the formation of α-migrating HDL by overexpression of human LCAT.

The FPLC analysis pointed out important differences in the HDL lipid profiles of the apoA-I mutants. On the basis of the HDL size, the lipid composition, the CE/TC ratio of the HDL region, the spherical shape of HDL, and the ratio of preβ1 to α-HDL, the helix 4P mutant (apoA-I[D102A/D103A]) appeared to be indistinguishable from WT apoA-I. Physicochemical studies have shown that this mutant undergoes a modest reduction in its α-helical content in both the lipid-free and lipid-bound state, and significant reduction in the cooperativity of unfolding in the lipid-free state. The stability of this mutant protein was altered moderately in the lipid-free state and significantly in the lipid-bound state (I. N. Gorshkova, A. Chroni, V. I. Zannis, and D. Atkinson, unpublished data).

Although both the helix 6P mutant (apoA-I[R160V/H162A]) and the helix 6Δ mutant {apoA-I[Δ(144−165)]} have very low LCAT activation capacity in vitro, they generated different phenotypes when they were expressed in apoA-I$^{-/-}$ mice. A distinct feature of the helix 6P mutant was the high apoA-I and phospholipid peak in the HDL_3 region, the diminished HDL cholesterol and cholesteryl ester peak, the low CE/TC ratio of HDL, the abundance of discoidal HDL, and the increased preβ1/α-HDL ratio. Most of the α-HDL in this mutant was in the form of small α3 HDL particles (*67*). On the basis of SDS−PAGE analysis of the fractions obtained from plasma of mice expressing the helix 6P mutant by density gradient ultracentrifugation and two-dimensional electrophoresis of the plasma, the HDL that was formed contained exclusively apoA-I but not apoE. In contrast, the helix 6Δ mutant had a very small peak of apoA-I, cholesterol, and phospholipids in the HDL region. In addition, this mutant promoted the formation of few spherical particles comparable in numbers to those seen in apoA-I$^{-/-}$ mice. The HDL particles formed had an increased preβ1/α-HDL ratio. Approximately two-thirds of the α-HDL generated by the helix 6Δ mutant was in the form of small α3 particles. Another difference between the helix 6P and helix 6Δ mutants was the effect of overexpression of LCAT on HDL levels. Coinfection of mice with adenoviruses expressing the helix 6P mutant and human LCAT caused a dramatic increase in HDL cholesterol and apoA-I levels. This treatment also converted the discoidal HDL into spherical α-HDL and increased the size of the α-HDL particles by converting the α3 to α2 and α1 particles. The preβ1/α-HDL ratio of mice expressing the helix 6P mutant and human LCAT is similar to that of mice expressing the WT apoA-I (compare Figure 3H and Figure 5N). On the other hand, coinfection of mice with adenoviruses expressing the helix 6Δ mutant caused an approximately 2.5-fold increase in the magnitude of the HDL cholesterol and apoA-I peak. This treatment also increased the number of spherical HDL particles, and converted all the preβ1-HDL into α-HDL particles.

An interesting observation of the LCAT treatment is that it normalized the CE/TC ratio in HDL and promoted the formation of spherical HDL particles not only in mice expressing WT and mutant apoA-I forms but also in the control mice expressing GFP. With one exception, which was the helix 6P mutant, the LCAT treatment increased the concentration of apoE and apoA-IV, and shifted the distribution of apoE toward the HDL_2 region and of apoA-IV toward the HDL_2 and HDL_3 region. These changes were also associated with the formation of large apoE-containing particles with fast electrophoretic mobility, as determined by two-dimensional gel electrophoresis. A plausible interpretation of these findings is that the excess of LCAT promoted the esterification of cholesterol of apoE- and apoA-IV-containing lipoprotein particles using apoE or apoA-IV as the LCAT activator (*68*−*70*), and thus promoted the formation of spherical particles containing these apolipoproteins. An increase in the plasma apoE level has also been observed in LCAT transgenic mice (*52*). In contrast to the control apoA-I$^{-/-}$ mice and those expressing WT or helix 4P and 6Δ mutant apoA-I forms, coinfection of mice with adenoviruses expressing the helix 6P mutant and human LCAT did not affect the plasma levels and the distribution of endogenous apoE and apoA-IV, and did not lead to the formation of apoE-containing lipoprotein particles as determined by two-dimensional gel electrophoresis. On the basis of SDS−PAGE analysis of the lipoprotein fractions obtained by density gradient ultracentrifugation of the plasma, it appears that the helix 6P mutant interfered with the formation of apoE- and apoA-IV-containing HDL size particles.

Molecular Mechanisms Causing HDL Deficiencies Due to Mutations in ApoA-I. This study indicates that residues 160 and/or 162 of apoA-I located in the hydrophilic face of helix 6 (*8*, *64*) play a crucial role in the activation of LCAT in vivo. Previous in vivo studies showed that the naturally occurring deletion mutant in helix 6 of apoA-I, apoA-I[Δ(146−160)], in human subjects (*15*) and a comparable deletion mutant, apoA-I[Δ(143−164)], in mice (*23*) reduced greatly the apoA-I and HDL levels (*15*, *23*). These studies did not provide a molecular explanation for what caused the reduction in the HDL level.

The phenotype generated by the R160V/H162A mutations mimics the phenotype of the classical LCAT deficiency in the sense that the mutant apoA-I drives the early steps in the biogenesis of HDL but blocks the esterification of free cholesterol that is present on the discoidal HDL particles and thus prevents the conversion of discoidal into spherical particles (Figure 6). Consistent with this interpretation are in vitro data showing that the helix 6P mutant has normal capacity to promote ABCA1-dependent cholesterol efflux (*65*), but it has a greatly reduced capacity to activate LCAT.

Our data indicate that the phenotypes created by the helix 6Δ mutant and helix 6P mutant are different. Like the helix 6P mutant, the helix 6Δ mutant has near-normal capacity to promote ABCA1-dependent lipid efflux in vitro (*65*). This implies that following binding to ABCA1, the helix 6Δ mutant may be lipidated and released normally from the apoA-I−ABCA1 complex (*65*). However, it appears that few of the lipidated apoA-I particles remain in the circulation and are able to mature into spherical HDL, even in the presence of excess LCAT. A potential reason for this finding can be obtained by comparison of the physicochemical properties of the WT apoA-I with the helix 6P and helix 6Δ mutants of apoA-I.

The α-helical content of WT and the helix 6Δ and 6P mutant apoA-I forms in the lipid-free state and on the rHDL particles was estimated from the normalized far-UV CD spectra. It was found that the helix 6Δ mutant had ap-

proximately 22 fewer residues in the α-helical conformation in the lipid-free state and had reduced chemical and thermal stability and cooperativity of unfolding as compared to the WT apoA-I. The deletion also caused a red shift in the wavelength of maximum fluorescence (*40*). In contrast, compared to WT apoA-I, the helix 6P mutant had normal helical content and stability, in both lipid-free and lipid-bound states, but had a statistically significant reduction in the cooperativity of thermal unfolding in the lipid-free state (I. N. Gorshkova, A. Chroni, V. I. Zannis, and D. Atkinson, unpublished data).

The very low catalytic efficiency of the enzyme in the presence of the helix 6P and 6Δ mutants observed in vitro and in vivo can be overcome by excess LCAT. This indicates that the endogenous mouse LCAT activity is limiting for the conversion of discoidal to spherical particles. Our data do now allow us to distinguish whether apoA-I participates in the catalytic mechanisms of LCAT, the binding of LCAT to HDL or rHDL containing apoA-I, or both. The role in the catalytic mechanism might involve, for instance, stabilization of the intermediates of the enzymatic reaction that proceeds via acylation and deacylation of the enzyme using lecithin as a substrate. On the other hand, the role in binding of LCAT to HDL may involve protein−protein interactions of the apoA-I bound on discoidal particles with LCAT and/or conformational changes in LCAT that may facilitate the catalysis.

In addition, the reduced stability of the helix 6Δ mutant may contribute to rapid in vivo catabolism and reduced levels of apoA-I and discoidal HDL substrate. The reduction in the substrate concentration, combined with changes in the catalytic efficiency of the enzyme caused by the helix 6Δ mutant, may explain the low levels of HDL, even in the presence of excess LCAT.

This study indicates that apoA-I point mutations in the general population may block the biogenesis of HDL at the level of conversion of the discoidal HDL particles to spherical and may cause pathologies similar to those observed in patients with classical LCAT deficiency or other HDL deficiencies.

ACKNOWLEDGMENT

We thank Dr. Silvia Santamarina-Fojo for providing the LCAT adenovirus, Ms. Gayle Forbes for technical assistance, and Ms. Anne Plunkett for typing the manuscript.

REFERENCES

1. Chroni, A., Liu, T., Gorshkova, I., Kan, H. Y., Uehara, Y., von Eckardstein, A., and Zannis, V. I. (2003) The central helices of apoA-I can promote ATP-binding cassette transporter A1 (ABCA1)-mediated lipid efflux. Amino acid residues 220−231 of the wild-type apoA-I are required for lipid efflux in vitro and high-density lipoprotein formation in vivo, *J. Biol. Chem. 278*, 6719−6730.
2. Laccotripe, M., Makrides, S. C., Jonas, A., and Zannis, V. I. (1997) The carboxyl-terminal hydrophobic residues of apolipoprotein A-I affect its rate of phospholipid binding and its association with high-density lipoprotein, *J. Biol. Chem. 272*, 17511−17522.
3. Liu, T., Krieger, M., Kan, H. Y., and Zannis, V. I. (2002) The effects of mutations in helices 4 and 6 of apoA-I on scavenger receptor class B type I (SR-BI)-mediated cholesterol efflux suggest that formation of a productive complex between reconstituted high-density lipoprotein and SR-BI is required for efficient lipid transport, *J. Biol. Chem. 277*, 21576−21584.
4. Zannis, V. I., Chroni, A., Kypreos, K. E., Kan, H. Y., Cesar, T. B., Zanni, E. E., and Kardassis, D. (2004) Probing the pathways of chylomicron and HDL metabolism using adenovirus-mediated gene transfer, *Curr. Opin. Lipidol. 15*, 151−166.
5. Nolte, R. T., and Atkinson, D. (1992) Conformational analysis of apolipoprotein A-I and E-3 based on primary sequence and circular dichroism, *Biophys. J. 63*, 1221−1239.
6. Borhani, D. W., Rogers, D. P., Engler, J. A., and Brouillette, C. G. (1997) Crystal structure of truncated human apolipoprotein A-I suggests a lipid-bound conformation, *Proc. Natl. Acad. Sci. U.S.A. 94*, 12291−12296.
7. Marcel, Y. L., and Kiss, R. S. (2003) Structure−function relationships of apolipoprotein A-I: A flexible protein with dynamic lipid associations, *Curr. Opin. Lipidol. 14*, 151−157.
8. Segrest, J. P., Li, L., Anantharamaiah, G. M., Harvey, S. C., Liadaki, K. N., and Zannis, V. (2000) Structure and function of apolipoprotein A-I and high-density lipoprotein, *Curr. Opin. Lipidol. 11*, 105−115.
9. Assmann, G., von Eckardstein, A., and Brewer, H. B. (2001) Familial analphalipoproteinemia: Tangier disease, in *The Metabolic and Molecular Basis of Inherited Disease* (Scriver, C. R., Beaudet, A. L., Sly, W. S., and Valle, D., Eds.) pp 2937−2960, McGraw-Hill, New York.
10. Soutar, A. K., Garner, C. W., Baker, H. N., Sparrow, J. T., Jackson, R. L., Gotto, A. M., and Smith, L. C. (1975) Effect of the human plasma apolipoproteins and phosphatidylcholine acyl donor on the activity of lecithin:cholesterol acyltransferase, *Biochemistry 14*, 3057−3064.
11. Acton, S., Rigotti, A., Landschulz, K. T., Xu, S., Hobbs, H. H., and Krieger, M. (1996) Identification of scavenger receptor SR-BI as a high-density lipoprotein receptor, *Science 271*, 518−520.
12. Krieger, M. (2001) Scavenger receptor class B type I is a multiligand HDL receptor that influences diverse physiologic systems, *J. Clin. Invest. 108*, 793−797.
13. Zannis, V. I., Kypreos, K. E., Chroni, A., Kardassis, D., and Zanni, E. E. (2004) Lipoproteins and atherogenesis, in *Molecular Mechanisms of Atherosclerosis* (Loscalzo, J., Ed.) pp 111−174, Taylor & Francis Books, London.
14. Matsunaga, T., Hiasa, Y., Yanagi, H., Maeda, T., Hattori, N., Yamakawa, K., Yamanouchi, Y., Tanaka, I., Obara, T., and Hamaguchi, H. (1991) Apolipoprotein A-I deficiency due to a codon 84 nonsense mutation of the apolipoprotein A-I gene, *Proc. Natl. Acad. Sci. U.S.A. 88*, 2793−2797.
15. Deeb, S. S., Cheung, M. C., Peng, R. L., Wolf, A. C., Stern, R., Albers, J. J., and Knopp, R. H. (1991) A mutation in the human apolipoprotein A-I gene. Dominant effect on the level and characteristics of plasma high-density lipoproteins, *J. Biol. Chem. 266*, 13654−13660.
16. Santamarina-Fojo, S., Hoeg, J. M., Assmann, G., and Brewer, H. B., Jr. (2001) Lecithin cholesterol acyltransferase deficiency and fish eye disease, in *The Metabolic and Molecular Bases of Inherited Disease* (Scriver, C. R., Beaudet, A. L., Sly, W. S., and Valle, D., Eds.) pp 2817−2834, McGraw-Hill, New York.
17. Frank, P. G., N'Guyen, D., Franklin, V., Neville, T., Desforges, M., Rassart, E., Sparks, D. L., and Marcel, Y. L. (1998) Importance of central α-helices of human apolipoprotein A-I in the maturation of high-density lipoproteins, *Biochemistry 37*, 13902−13909.
18. Minnich, A., Collet, X., Roghani, A., Cladaras, C., Hamilton, R. L., Fielding, C. J., and Zannis, V. I. (1992) Site-directed mutagenesis and structure−function analysis of the human apolipoprotein A-I. Relation between lecithin-cholesterol acyltransferase activation and lipid binding, *J. Biol. Chem. 267*, 16553−16560.
19. Sorci-Thomas, M., Kearns, M. W., and Lee, J. P. (1993) Apolipoprotein A-I domains involved in lecithin-cholesterol acyltransferase activation. Structure:function relationships, *J. Biol. Chem. 268*, 21403−21409.
20. Sorci-Thomas, M. G., Curtiss, L., Parks, J. S., Thomas, M. J., and Kearns, M. W. (1997) Alteration in apolipoprotein A-I 22-mer repeat order results in a decrease in lecithin:cholesterol acyltransferase reactivity, *J. Biol. Chem. 272*, 7278−7284.
21. Dhoest, A., Zhao, Z., De Geest, B., Deridder, E., Sillen, A., Engelborghs, Y., Collen, D., and Holvoet, P. (1997) Role of the Arg123-Tyr166 paired helix of apolipoprotein A-I in lecithin: cholesterol acyltransferase activation, *J. Biol. Chem. 272*, 15967−15972.
22. Lindholm, E. M., Bielicki, J. K., Curtiss, L. K., Rubin, E. M., and Forte, T. M. (1998) Deletion of amino acids Glu146→Arg160 in human apolipoprotein A-I (ApoA-ISeattle) alters lecithin:

cholesterol acyltransferase activity and recruitment of cell phospholipid, *Biochemistry 37*, 4863−4868.
23. Sorci-Thomas, M. G., Thomas, M., Curtiss, L., and Landrum, M. (2000) Single repeat deletion in ApoA-I blocks cholesterol esterification and results in rapid catabolism of delta6 and wild-type ApoA-I in transgenic mice, *J. Biol. Chem. 275*, 12156−12163.
24. Hoang, A., Huang, W., Sasaki, J., and Sviridov, D. (2003) Natural mutations of apolipoprotein A-I impairing activation of lecithin: cholesterol acyltransferase, *Biochim. Biophys. Acta 1631*, 72−76.
25. McManus, D. C., Scott, B. R., Frank, P. G., Franklin, V., Schultz, J. R., and Marcel, Y. L. (2000) Distinct central amphipathic α-helices in apolipoprotein A-I contribute to the in vivo maturation of high-density lipoprotein by either activating lecithin-cholesterol acyltransferase or binding lipids, *J. Biol. Chem. 275*, 5043−5051.
26. Scott, B. R., McManus, D. C., Franklin, V., McKenzie, A. G., Neville, T., Sparks, D. L., and Marcel, Y. L. (2001) The N-terminal globular domain and the first class A amphipathic helix of apolipoprotein A-I are important for lecithin:cholesterol acyltransferase activation and the maturation of high-density lipoprotein in vivo, *J. Biol. Chem. 276*, 48716−48724.
27. Chroni, A., Kan, H. Y., Shkodrani, A., Liu, T., and Zannis, V. I. (2005) Deletions of Helices 2 and 3 of Human ApoA-I Are Associated with Severe Dyslipidemia following Adenovirus-Mediated Gene Transfer in ApoA-I-Deficient Mice, *Biochemistry 44*, 4108−4117.
28. Reardon, C. A., Kan, H. Y., Cabana, V., Blachowicz, L., Lukens, J. R., Wu, Q., Liadaki, K., Getz, G. S., and Zannis, V. I. (2001) In vivo studies of HDL assembly and metabolism using adenovirus-mediated transfer of ApoA-I mutants in ApoA-I-deficient mice, *Biochemistry 40*, 13670−13680.
29. Liu, T. (2002) Structural and functional analysis of human apolipoprotein A-I, Ph.D. Thesis, Department of Biochemistry, Boston University School of Medicine, Boston, MA.
30. Moriyama, K., Sasaki, J., Matsunaga, A., Takada, Y., Kagimoto, M., and Arakawa, K. (1996) Identification of two apolipoprotein variants, A-I Karatsu (Tyr 100→His) and A-I Kurume (His 162→Gln), *Clin. Genet. 49*, 79−84.
31. Miettinen, H. E., Gylling, H., Miettinen, T. A., Viikari, J., Paulin, L., and Kontula, K. (1997) Apolipoprotein A-IFin. Dominantly inherited hypoalphalipoproteinemia due to a single base substitution in the apolipoprotein A-I gene, *Arterioscler. Thromb. Vasc. Biol. 17*, 83−90.
32. Miettinen, H. E., Jauhiainen, M., Gylling, H., Ehnholm, S., Palomaki, A., Miettinen, T. A., and Kontula, K. (1997) Apolipoprotein A-IFIN (Leu159→Arg) mutation affects lecithin cholesterol acyltransferase activation and subclass distribution of HDL but not cholesterol efflux from fibroblasts, *Arterioscler. Thromb. Vasc. Biol. 17*, 3021−3032.
33. Leren, T. P., Bakken, K. S., Daum, U., Ose, L., Berg, K., Assmann, G., and von Eckardstein, A. (1997) Heterozygosity for apolipoprotein A-I(R160L)Oslo is associated with low levels of high-density lipoprotein cholesterol and HDL-subclass LpA-I/A-II but normal levels of HDL-subclass LpA-I, *J. Lipid Res. 38*, 121−131.
34. Huang, W., Sasaki, J., Matsunaga, A., Nanimatsu, H., Moriyama, K., Han, H., Kugi, M., Koga, T., Yamaguchi, K., and Arakawa, K. (1998) A novel homozygous missense mutation in the apo A-I gene with apo A-I deficiency, *Arterioscler. Thromb. Vasc. Biol. 18*, 389−396.
35. McManus, D. C., Scott, B. R., Franklin, V., Sparks, D. L., and Marcel, Y. L. (2001) Proteolytic degradation and impaired secretion of an apolipoprotein A-I mutant associated with dominantly inherited hypoalphalipoproteinemia, *J. Biol. Chem. 276*, 21292−21302.
36. Martin-Campos, J. M., Julve, J., Escola, J. C., Ordonez-Llanos, J., Gomez, J., Binimelis, J., Gonzalez-Sastre, F., and Blanco-Vaca, F. (2002) ApoA-I(MALLORCA) impairs LCAT activation and induces dominant familial hypoalphalipoproteinemia, *J. Lipid Res. 43*, 115−123.
37. Miller, M., Aiello, D., Pritchard, H., Friel, G., and Zeller, K. (1998) Apolipoprotein A-I(Zavalla) (Leu159→Pro): HDL cholesterol deficiency in a kindred associated with premature coronary artery disease, *Arterioscler. Thromb. Vasc. Biol. 18*, 1242−1247.
38. Chroni, A., Kan, H. Y., Kypreos, K. E., Gorshkova, I. N., Shkodrani, A., and Zannis, V. I. (2004) Substitutions of glutamate 110 and 111 in the middle helix 4 of human apolipoprotein A-I (apoA-I) by alanine affect the structure and in vitro functions of apoA-I and induce severe hypertriglyceridemia in apoA-I-deficient mice, *Biochemistry 43*, 10442−10457.
39. Roghani, A., and Zannis, V. I. (1988) Alterations of the glutamine residues of human apolipoprotein AI propeptide by in vitro mutagenesis. Characterization of the normal and mutant protein forms, *Biochemistry 27*, 7428−7435.
40. Gorshkova, I. N., Liu, T., Zannis, V. I., and Atkinson, D. (2002) Lipid-free structure and stability of apolipoprotein A-I: Probing the central region by mutation, *Biochemistry 41*, 10529−10539.
41. Williamson, R., Lee, D., Hagaman, J., and Maeda, N. (1992) Marked reduction of high density lipoprotein cholesterol in mice genetically modified to lack apolipoprotein A-I, *Proc. Natl. Acad. Sci. U.S.A. 89*, 7134−7138.
42. Fielding, C. J., and Fielding, P. E. (1996) Two-dimensional nondenaturing electrophoresis of lipoproteins: Applications to high-density lipoprotein speciation, *Methods Enzymol. 263*, 251−259.
43. Hill, J. S., O, K., Wang, X., Paranjape, S., Dimitrijevich, D., Lacko, A. G., and Pritchard, P. H. (1993) Expression and characterization of recombinant human lecithin:cholesterol acyltransferase, *J. Lipid Res. 34*, 1245−1251.
44. Jin, L., Lee, Y. P., and Jonas, A. (1997) Biochemical and biophysical characterization of human recombinant lecithin: cholesterol acyltransferase, *J. Lipid Res. 38*, 1085−1093.
45. Amar, M. J. A., Shamburek, R. D., Foger, B., Hoyt, R. F., Wood, D. O., Santamarina-Fojo, S., and Brewer, H. B. (1998) Adenovirus-mediated expression of LCAT in non-human primates leads to an antiatherogenic lipoprotein profile with increased HDL and decreased LDL, *Circ. Suppl. 98*, I-35.
46. Matz, C. E., and Jonas, A. (1982) Micellar complexes of human apolipoprotein A-I with phosphatidylcholines and cholesterol prepared from cholate-lipid dispersions, *J. Biol. Chem. 257*, 4535−4540.
47. Sorci-Thomas, M. G., Curtiss, L., Parks, J. S., Thomas, M. J., Kearns, M. W., and Landrum, M. (1998) The hydrophobic face orientation of apolipoprotein A-I amphipathic helix domain 143−164 regulates lecithin:cholesterol acyltransferase activation, *J. Biol. Chem. 273*, 11776−11782.
48. Roosbeek, S., Vanloo, B., Duverger, N., Caster, H., Breyne, J., De, B. I., Patel, H., Vandekerckhove, J., Shoulders, C., Rosseneu, M., and Peelman, F. (2001) Three arginine residues in apolipoprotein A-I are critical for activation of lecithin:cholesterol acyltransferase, *J. Lipid Res. 42*, 31−40.
49. Cho, K. H., Durbin, D. M., and Jonas, A. (2001) Role of individual amino acids of apolipoprotein A-I in the activation of lecithin: cholesterol acyltransferase and in HDL rearrangements, *J. Lipid Res. 42*, 379−389.
50. Sorci-Thomas, M. G., and Thomas, M. J. (2002) The effects of altered apolipoprotein A-I structure on plasma HDL concentration, *Trends Cardiovasc. Med. 12*, 121−128.
51. Zhao, Y., Thorngate, F. E., Weisgraber, K. H., Williams, D. L., and Parks, J. S. (2005) Apolipoprotein E is the major physiological activator of lecithin-cholesterol acyltransferase (LCAT) on apolipoprotein B lipoproteins, *Biochemistry 44*, 1013−1025.
52. Vaisman, B. L., Klein, H. G., Rouis, M., Berard, A. M., Kindt, M. R., Talley, G. D., Meyn, S. M., Hoyt, R. F., Jr., Marcovina, S. M., Albers, J. J., Hoeg, J. M., Brewer, H. B., and Santamarina-Fojo, S. (1995) Overexpression of human lecithin cholesterol acyltransferase leads to hyperalphalipoproteinemia in transgenic mice, *J. Biol. Chem. 270*, 12269−12275.
53. Fielding, C. J., Shore, V. G., and Fielding, P. E. (1972) A protein cofactor of lecithin:cholesterol acyltransferase, *Biochem. Biophys. Res. Commun. 46*, 1493−1498.
54. Sparks, D. L., Frank, P. G., Braschi, S., Neville, T. A., and Marcel, Y. L. (1999) Effect of apolipoprotein A-I lipidation on the formation and function of pre-β and α-migrating LpA-I particles, *Biochemistry 38*, 1727−1735.
55. Daum, U., Leren, T. P., Langer, C., Chirazi, A., Cullen, P., Pritchard, P. H., Assmann, G., and von Eckardstein, A. (1999) Multiple dysfunctions of two apolipoprotein A-I variants, apoA-I(R160L)Oslo and apoA-I(P165R), that are associated with hypoalphalipoproteinemia in heterozygous carriers, *J. Lipid Res. 40*, 486−494.
56. Araki, K., Sasaki, J., Matsunaga, A., Takada, Y., Moriyama, K., Hidaka, K., and Arakawa, K. (1994) Characterization of two new human apolipoprotein A-I variants: Apolipoprotein A-I Tsushima (Trp-108→Arg) and A-I Hita (Ala-95→Asp), *Biochim. Biophys. Acta 1214*, 272−278.

57. Takada, Y., Sasaki, J., Ogata, S., Nakanishi, T., Ikehara, Y., and Arakawa, K. (1990) Isolation and characterization of human apolipoprotein A-I Fukuoka (110 Glu→Lys). A novel apolipoprotein variant, *Biochim. Biophys. Acta 1043*, 169−176.
58. Sviridov, D., Pyle, L. E., Jauhiainen, M., Ehnholm, C., and Fidge, N. H. (2000) Deletion of the propeptide of apolipoprotein A-I reduces protein expression but stimulates effective conversion of preβ-high-density lipoprotein to α-high-density lipoprotein, *J. Lipid Res. 41*, 1872−1882.
59. Sviridov, D., Hoang, A., Sawyer, W. H., and Fidge, N. H. (2000) Identification of a sequence of apolipoprotein A-I associated with the activation of lecithin:cholesterol acyltransferase, *J. Biol. Chem. 275*, 19707−19712.
60. Cho, K. H., and Jonas, A. (2000) A key point mutation (V156E) affects the structure and functions of human apolipoprotein A-I, *J. Biol. Chem. 275*, 26821−26827.
61. Romling, R., von Eckardstein, A., Funke, H., Motti, C., Fragiacomo, G. C., Noseda, G., and Assmann, G. (1994) A nonsense mutation in the apolipoprotein A-I gene is associated with high-density lipoprotein deficiency and periorbital xanthelasmas, *Arterioscler. Thromb. 14*, 1915−1922.
62. Daum, U., Langer, C., Duverger, N., Emmanuel, F., Benoit, P., Denefle, P., Chirazi, A., Cullen, P., Pritchard, P. H., Bruckert, E., Assmann, G., and von Eckardstein, A. (1999) Apolipoprotein A-I (R151C)Paris is defective in activation of lecithin:cholesterol acyltransferase but not in initial lipid binding, formation of reconstituted lipoproteins, or promotion of cholesterol efflux, *J. Mol. Med. 77*, 614−622.
63. Bruckert, E., von Eckardstein, A., Funke, H., Beucler, I., Wiebusch, H., Turpin, G., and Assmann, G. (1997) The replacement of arginine by cysteine at residue 151 in apolipoprotein A-I produces a phenotype similar to that of apolipoprotein A-IMilano, *Atherosclerosis 128*, 121−128.
64. Segrest, J. P., Jones, M. K., Klon, A. E., Sheldahl, C. J., Hellinger, M., De Loof, H., and Harvey, S. C. (1999) A detailed molecular belt model for apolipoprotein A-I in discoidal high-density lipoprotein, *J. Biol. Chem. 274*, 31755−31758.
65. Chroni, A., Liu, T., Fitzgerald, M. L., Freeman, M. W., and Zannis, V. I. (2004) Cross-linking and lipid efflux properties of apoA-I mutants suggest direct association between apoA-I helices and ABCA1, *Biochemistry 43*, 2126−2139.
66. Fitzgerald, M. L., Morris, A. L., Chroni, A., Mendez, A. J., Zannis, V. I., and Freeman, M. W. (2004) ABCA1 and amphipathic apolipoproteins form high-affinity molecular complexes required for cholesterol efflux, *J. Lipid Res. 45*, 287−294.
67. Asztalos, B. F., and Schaefer, E. J. (2003) High-density lipoprotein subpopulations in pathologic conditions, *Am. J. Cardiol. 91*, 12E−17E.
68. Steinmetz, A., Kaffarnik, H., and Utermann, G. (1985) Activation of phosphatidylcholine-sterol acyltransferase by human apolipoprotein E isoforms, *Eur. J. Biochem. 152*, 747−751.
69. Chen, C. H., and Albers, J. J. (1985) Activation of lecithin: cholesterol acyltransferase by apolipoproteins E-2, E-3, and A-IV isolated from human plasma, *Biochim. Biophys. Acta 836*, 279−285.
70. Steinmetz, A., and Utermann, G. (1985) Activation of lecithin: cholesterol acyltransferase by human apolipoprotein A-IV, *J. Biol. Chem. 260*, 2258−2264.
71. Karathanasis, S. K., Salmon, E., Haddad, I. A., and Zannis, V. I. (1985) in *Biochemistry and Biology of Plasma Proteins* (Scanu, A. M., and Spector, A. A., Eds.) pp 474−493, Marcel Dekker, New York.
72. Rubin, E. M., Ishida, B. Y., Clift, S. M., and Krauss, R. M. (1991) Expression of human apolipoprotein A-I in transgenic mice results in reduced plasma levels of murine apolipoprotein A-I and the appearance of two new high-density lipoprotein size subclasses, *Proc. Natl. Acad. Sci. U.S.A. 88*, 434−438.

BI050962O